



THE UNIVERSITY *of* EDINBURGH

Edinburgh Research Explorer

Orthogonal Selection and Fixing of Coordination Self-Assembly Pathways for Robust Metallo-organic Ensemble Construction

Citation for published version:

Burke, MJ, Nichol, GS & Lusby, PJ 2016, 'Orthogonal Selection and Fixing of Coordination Self-Assembly Pathways for Robust Metallo-organic Ensemble Construction', *Journal of the American Chemical Society*, vol. 138, no. 29, pp. 9308-9315. <https://doi.org/10.1021/jacs.6b05364>

Digital Object Identifier (DOI):

[10.1021/jacs.6b05364](https://doi.org/10.1021/jacs.6b05364)

Link:

[Link to publication record in Edinburgh Research Explorer](#)

Document Version:

Peer reviewed version

Published In:

Journal of the American Chemical Society

General rights

Copyright for the publications made accessible via the Edinburgh Research Explorer is retained by the author(s) and / or other copyright owners and it is a condition of accessing these publications that users recognise and abide by the legal requirements associated with these rights.

Take down policy

The University of Edinburgh has made every reasonable effort to ensure that Edinburgh Research Explorer content complies with UK legislation. If you believe that the public display of this file breaches copyright please contact openaccess@ed.ac.uk providing details, and we will remove access to the work immediately and investigate your claim.



Orthogonal Selection and Fixing of Coordination Self-Assembly Pathways for Robust Metallo-Organic Ensemble Construction

Michael J. Burke, Gary S. Nichol and Paul J. Lusby*

EaStCHEM School of Chemistry, University of Edinburgh, Joseph Black Building, David Brewster Road, Edinburgh, Scotland, UK. EH9 3FJ. E-mail: Paul.Lusby@ed.ac.uk

ABSTRACT: Supramolecular construction strategies have overwhelmingly relied on the principles of thermodynamic control. While this approach has yielded an incredibly diverse and striking collection of ensembles, there are downsides, most obviously the necessity to trade-off reversibility against structural integrity. Herein we describe an alternative “assembly-followed-by-fixing” approach that possesses the high-yielding, atom-efficient advantages of reversible self-assembly reactions, yet gives structures that possess a covalent-like level of kinetic robustness. We have chosen to exemplify these principles in the preparation of a series of M_2L_3 helicates and M_4L_6 tetrahedra. While the rigidity of various bis(bidentate) ligands cause the larger species to be energetically preferred, we are able to freeze the self-assembly process under “non-ambient” conditions, to selectivity give the disfavored M_2L_3 helicates. We also demonstrate “kinetic-stimuli” (redox and light) induced switching between architectures, notably reconstituting the lower energy tetrahedra into highly-distorted helicates.

Introduction

Discrete supramolecular constructs continue to provide notable interest because of the myriad applications from medicine¹ through catalysis² to storage and protection³. The discovery of these functional properties has been enabled by straight-forward, high-yielding synthetic methodology, which has permitted access to a wide and diverse set of architectures. The mainstay of these synthetic methods has been thermodynamically-controlled self-assembly protocols,⁴ and in this regard certain metal-ligand interactions are ideally suited,⁵ providing an appropriate balance between strength—ensuring that closed systems are energetically favored over a wide range of concentrations—and reversibility, which allows the necessary exploration of the potential energy landscape. However, this method and the systems it produces are not without drawbacks. Firstly, the thermodynamic selectivity for a particular species may sometimes be poor, as can be the case for square-triangle equilibria.⁶ While finely-balanced equilibria are interesting from a fundamental supramolecular or system’s perspective, and can be readily exploited as adaptive chemical entities⁷ the isolation of an individual component from a supramolecular product mixture can be highly challenging, if not impossible. Even with systems where a thermodynamic sink leads to a single product, the reversibility of metal-ligand interactions can still limit assembly integrity to rather specific “ambient” conditions, and this is despite the inherent kinetic stabilization that most metallocupramolecular species exhibit due to cooperative chelate effects.⁸

Chemical locking provides an ideal strategy to overcome the problems associated with weak interactions,⁹ allowing systems to be “fixed” at a given equilibrium position. Similar strategies are widespread for dynamic covalent chemistry (DCC) where reversible reactions are often made non-labile by changing conditions, post-assembly modification or through removal of a catalyst.¹⁰ While DCC has been used widely to give

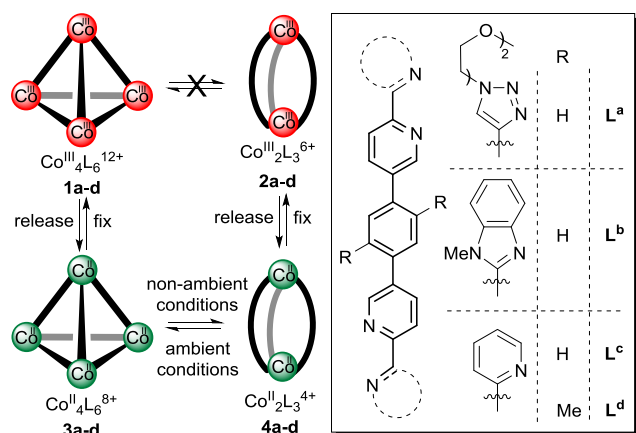
high-yielding access to complex yet often robust organic scaffolds, such as interlocked architectures¹¹ or cages¹², more recently the interconversion between dynamic and non-dynamic states has been exploited to create molecular devices using orthogonal pairs of responsive covalent bonds.¹³

In the context of metallocupramolecular species, the most widely used strategy to create kinetically stable ensembles has been to exploit non-labile metal ions,¹⁴ most commonly 2nd and 3rd row d-block elements,¹⁵ which only become dynamic at elevated temperature. One of the earliest as well as elegant and striking examples of this was Fujita’s isolation of a Pt catenane—particularly notable because this topologically non-trivial species appears thermodynamically non-favored under “standard” conditions.^{15a} The main problem, however, with using temperature as a “kinetic stimulus” is that it is non-selective with respect to the thermodynamics of any given system because it additionally perturbs any equilibrium where $\Delta S \neq 0$. Also, the use of non-labile metal ions can lead to low yields or kinetically trapped intermediates.^{1a,14e,16} The Fujita group have sought to overcome these issues through the application of solvochemical methods¹⁷ and light¹⁸, which serve as “kinetic-stimuli” to activate otherwise non-labile interactions. The use of light—which functions by switching the mechanism of Pt-substitution reactions¹⁸—is particularly notable because this kinetic-activation is orthogonal to the thermodynamics of the system. Despite the elegance and benefits of this approach, this light-activated assembly procedure has not become widespread having been limited (as far as we are aware) to the preparation of a metallocupramolecular catenane,^{18a} a triangle^{18b} and a single hexanuclear octagonal cage.^{18b}

Recently, we targeted an oxidative deactivation strategy for accessing robust coordination assemblies.¹⁹ This method utilizes the substitutional non-lability of Co^{III} in comparison to Co^{II}.²⁰ This approach possesses many benefits, such as atom efficiency, high yields and operational simplicity. At the same time it produces robust products and exploits a cheap,

abundant, less-toxic first row transition metal. Using a series of rigid bis(*N,N*-chelates) to demonstrate generality, we now develop this approach much further by showing that in addition to the preferred tetrahedra, **1a-d**, we can also adapt the reaction to give the highly distorted helicates, **2a-d**, with complete selectivity (Scheme 1). These higher energy species, **2a-d**, would be otherwise difficult to isolate with a non-locked system.²¹ We also show that the system dynamics can be switched back on using both redox and photoredox-based stimuli. These have been applied to interconvert different assemblies, most notably reconstituting tetrahedra into helicates thus moving energetically uphill. Mechanisms that allow the potential energy landscape to be traversed using ratcheting inputs are important to fields such as molecular machines and motors.²²

Scheme 1. Selective synthesis of kinetically robust tetrahedra and helicates using an “assembly-followed-by-fixing” method.



Results and Discussion

Pre-oxidation Co^{II} Equilibrium and Variable Oxidation Rate Studies. **1a** was previously obtained as a single species when cerium ammonium nitrate (CAN) was added dropwise to a 3:2 mol ratio of **L^a** and Co(ClO₄)₂·6H₂O in CH₃CN at RT.¹⁹ To determine whether the single fixed product is representative of the dynamic state, we decided to investigate the equilibrium between **L^a** and Co(ClO₄)₂·6H₂O in CD₃CN using ¹H NMR spectroscopy (Figure 1). Interestingly, a solution at a concentration typical of the assembly-followed-by-fixing method ([Co^{II}]_{total} = 11.7 mM) showed two paramagnetically shifted species (Figure 1a). This likely indicates a Co^{II} equilibrium between species of formulae (M₂L₃)_n,^{7,21a,b,23} most obviously tetrahedron **3a** and helicate **4a**. This assignment is supported by a significant change in speciation following multiple dilutions of the stock **L^a**/Co^{II} solution (Figures 1 b, d–f), which overall showed an increase in **4a** and a concomitant decrease in **3a** at lower concentrations. The rate of re-equilibration also occurred quickly; steady concentrations were reached within minutes of dilution, hence explaining why only **4a** was observed using the dilute conditions required for analysis by Electrospray Ionization Mass Spectrometry (ESI-MS). A similar thermodynamic switch was also observed at elevated temperature (Figure 1c), wherein the entropically favored **4a** (blue) increases at the expense of **3a** (red).

An implication of the Co^{II} equilibrium experiments were that dropwise addition of CAN to a mixture of **3a** and **4a** induces a helicate to tetrahedron constitutional rearrangement. We chose to further investigate by varying the rate of oxidant

addition with the ratio of **3a**:**4a** almost equal (55:45; [Co^{II}]_{total} = 5.56 mM; Table 1). This clearly confirmed that slow addition causes transformation into the larger species. It is interesting to note that the low [Co^{II}]_{total} towards the end of the fixing process should bias the equilibrium towards **4a**. Nonetheless, the slowest fixing reaction is completely selective for **1a**. An explanation for this could be the stronger preference of d⁶ Co^{III} for octahedral coordination geometry, wherein a small amount of Co^{III} “seeds” shift the equilibrium towards tetrahedral species. In contrast, when CAN is added rapidly to a vigorously stirred solution, the fixed product ratio (**1a**:**2a**) reflects the dynamic state (**3a**:**4a**) within error of NMR integrations. Overall, it is interesting to compare the effects of slow and fast CAN addition; slow addition perturbs the bias of the system whereas rapid oxidation fixes the dynamics without changing the thermodynamic distribution.

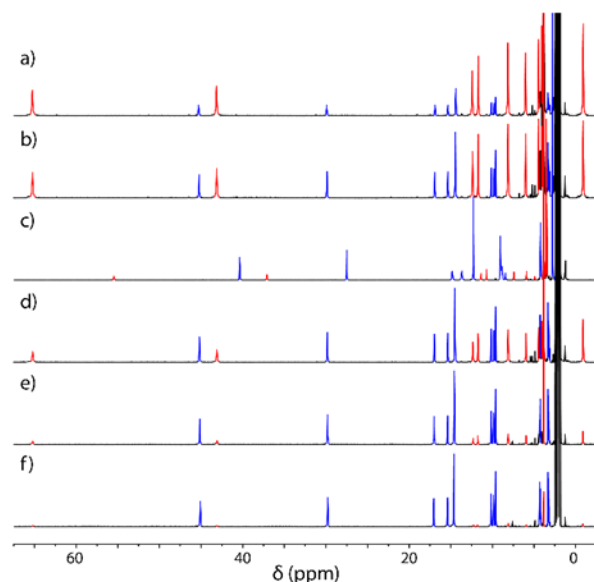
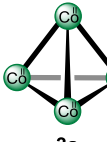

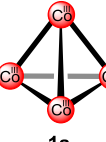



Figure 1. Partial ¹H NMR spectra (500 MHz, CD₃CN, 300 K unless stated) showing the equilibrium between **4a** (blue) and **3a** (red) as a function of [Co^{II}]_{total} and temperature. a) 11.7 mM; b) 5.84 mM; c) 5.84 mM @ 343 K; d) 2.92 mM; e) 1.46 mM; f) 0.73 mM.

Table 1. Variation in fixed product ratio **1a:**2a** as a function of rate of oxidant addition.^{a,b}**

				
CAN total addition time	< 5 sec	22 min ^c	110 min ^c	18 h 20 min ^c
1a : 2a ratio	51:49	87:13	95:5	99:1

^aReaction conditions: [Co^{II}]_{total} = 5.56 mM, 1.5 eq. **L^a**, CH₃CN, 50 °C, 30 min, then CAN added at RT as a 11.7 mM CH₃CN solution; ^bInitial mol ratio of **3a**:**4a** = 55:45; ^cCAN added at a constant rate using a syringe pump.

Selective Co^{III} Helicate and Tetrahedron Synthesis. Even though **4a** is only preferred under dilute conditions, the capacity to fix the Co^{II} equilibrium without perturbation allowed **2a** to be isolated as a single species. This was achieved

by adding CAN rapidly to a vigorously stirred, dilute solution of **L^a** and $\text{Co}(\text{ClO}_4)_2 \cdot 6\text{H}_2\text{O}$ ($[\text{Co}^{\text{II}}]_{\text{total}} = 0.1 \text{ mM}$), from which **2a**·6PF₆ was obtained in 93% yield. Even with ligands that show a greater thermodynamic preference for Co^{II} tetrahedra, as is the case with **L^{b-d}** (See Supporting Information, Section 3), the fixing reactions could be optimized to selectively give only Co^{III} helicates **2b-d** (with isolated yields of 93% 88% and 64%, respectively). This is best exemplified with **2d**. The ¹H NMR spectra of the Co^{II} equilibrium revealed a much stronger bias towards **3d** (Figure S5); even under dilute conditions ($[\text{Co}^{\text{II}}]_{\text{total}} = 0.73 \text{ mM}$) the mol ratio of **3d:4d** was 62:38 (c.f. the mol ratio of **3a:4a** was 4:96 at the same concentration). Nonetheless, oxidizing a very dilute solution of Co^{II} and **L^d** ($[\text{Co}^{\text{II}}]_{\text{total}} = 35 \text{ }\mu\text{M}$) gave **2d** as a single species. With the bipy ligands, **L^{c-d}**, we also observed that the Co^{II} states are much less dynamic, with equilibration of **3c:4c** taking a week at room temperature (Figure S4). Long reaction times could be avoided, however, by adding the ligands to a very dilute solution of Co^{II}. When these reactions were oxidized immediately after ligand dissolution (ca. 1 h @ 50 °C), **2c-d** were obtained exclusively. With these reactions it is likely that **4c-d** are formed directly under kinetic control thereby avoiding slow rearrangement from **3c-d**. The Co^{III} helicates **2a-d** have all been characterized by NMR and ESI-MS. In addition, the structures of **2c** and **2d** have been confirmed by X-ray crystallography (Figure 2b, d). The Co-N bond lengths are all what would be expected for Co^{III} (1.92–1.95 Å). Also, there is significant distortion to accommodate the closed structures, however, this appears to be manifested mainly in bending to the ligand frameworks, as both structures showed Co^{III} adopts close to ideal octahedral geometry.²⁴

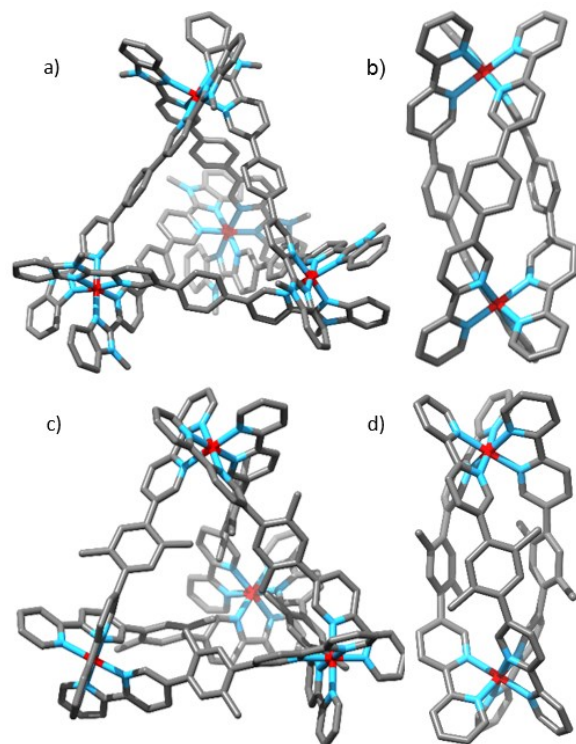


Figure 2. X-ray crystal structures (hydrogen atoms, counteranions and solvent omitted for clarity) of a) **1b**; b) **2c**; c) **1d** and d) **2d** (color code: carbon, grey; nitrogen, blue; cobalt, red).

Co^{III} tetrahedra, **1b-d**, were also selectively obtained starting from **L^{b-d}**. While the preceding Co^{II} equilibria all favor

these larger species (see above), dropwise addition of the oxidant had a much less pronounced effect (See Supporting Information, Section 4). Indeed, variable oxidation rate studies, analogous to those with **L^a** (e.g. Table 1), showed only a marginal increase in the proportion of **1c** when CAN was added very slowly to a mixture of **3c** and **4c** (Table S1). This is consistent with the slower equilibration of bipy-based Co^{II} assemblies (see above). Nonetheless, the PF₆ salts of **1b-d** were isolated as single compounds in yields of 78%, 77% and 83% respectively. As well as the relevant spectroscopic characterization, the structures of **1b** and **1d** have been confirmed by X-ray crystallography as homochiral *T* symmetric architectures (Figure 2a, c).²⁵

Kinetic Robustness as a Function of Ligand Type.

The Co^{III} coordination assemblies that feature the 2-(*N*-methylbenzimidazole)pyridyl, and even more so 2,2'-bipy chelates, show enhanced kinetic robustness in comparison to those formed from the pyridyl-triazole ligand **L^a**, as evidenced by the stability of the helicates **2a-d** in solution (see Supporting Information Section 5). While **2a** appears stable for weeks at room temperature in CD₃CN, when the sample is heated, slow yet complete rearrangement to **1a** is observed by ¹H NMR spectroscopy, with this taking one week at 40 °C and then another week at 50 °C, followed by 2 days at 60 °C (Figure S9). This transformation also indicates that, as expected, **1a** is energetically preferred in comparison to **2a**, further confirming that the assembly-followed-by-fixing method is able to trap species that are thermodynamically disfavored. In contrast, **2c** doesn't show any signs of change when heated for a week each at 40, 50, 60 and then 70 °C (**2b**, shows intermediate stability, showing complete conversion to tetrahedron following 6 days at the 60 °C stage; Figures S10 and S11). These results indicate that the kinetic stability of **2a-c** qualitatively match the dynamics of the Co^{II} state with ligands **L^{a-c}**. A comparison of the bipy-based helicates (**2c** vs. **2d**) reveals that, as perhaps could be anticipated, the increased steric bulk marginally reduces the kinetic stability, with slight conversion to **1d** observed after the same heating regime (Figure S12).

Kinetic-Stimuli Induced Switching of Coordination Architectures. As none of the Co^{III} helicates **2a-d** rearrange to their corresponding tetrahedra **1a-d** at room temperature, we concluded that this transformation could be readily used to probe the switching between locked and unlocked states. While metallosupramolecular transformations have become increasingly common,^{7,23a,d-j,26} these have overwhelmingly utilized stimuli that achieve switching by altering the thermodynamic preference of the system. In contrast we sought to manipulate through a different mechanism—by selectively revealing a lower barrier between energy minima (Figure 3) rather than by altering the relative depths of the energy wells on the potential energy surface. Initially focusing on the more robust helicates **2b** and **2c**, we were pleased to observe that when a slight excess of tetrabutylammonium iodide (TBAI) was added, the ¹H NMR spectra revealed the loss of the starting material resonances and the appearance of paramagnetically shifted signals (Figures S13 and S14), indicating the formation of Co^{II} complexes. In the case of **2c**, the predominant species formed was the metastable **4c** (Figure S14b), which over 5 days at room temperature was gradually replaced by **3c** (Figure S14c). Dropwise addition of CAN to the equilibrated Co^{II} samples gave exclusively **1b** and predominantly **1c** (Figures S13d and S14d). Starting far away from equilibrium we can utilize stimuli that mainly affect the dynamics of ligand exchange to

bring about this transformation selectively at ambient temperatures (Scheme 2, Method 1; Figure 3).

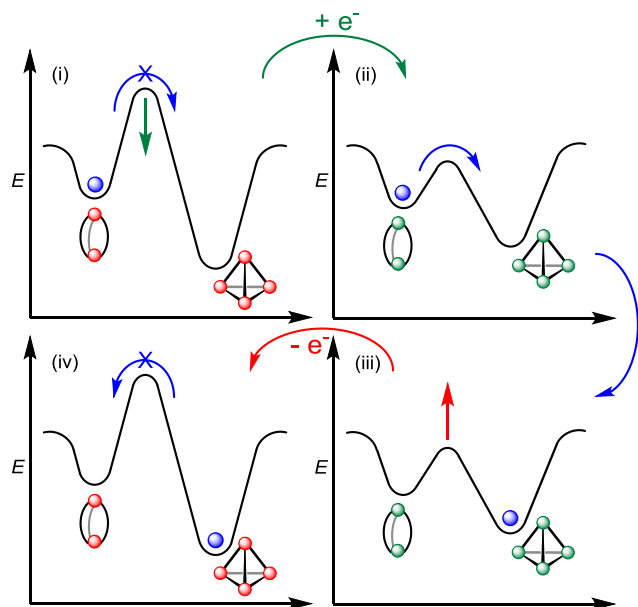
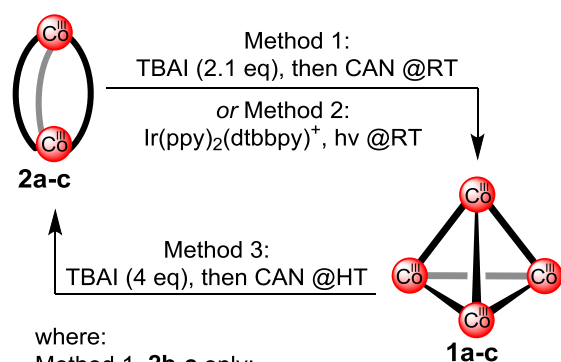


Figure 3. Energy profile diagrams showing a generic, kinetic-stimuli-induced helicate to tetrahedron transformation.

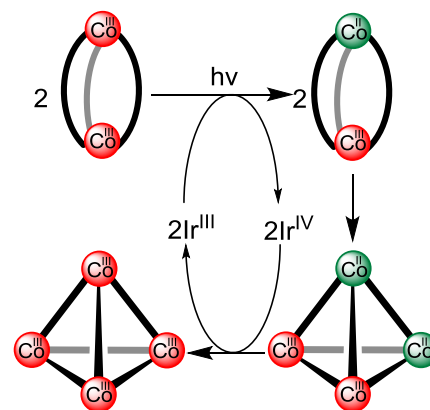
Scheme 2. “Kinetic Stimuli-induced” assembly interconversions.



We have also explored the use of photoredox methods, which are currently enjoying a renaissance in organic synthetic applications,²⁷ for transforming the helicates into tetrahedral species. In this case we envisaged that a low steady state concentration of Co^{II} species would facilitate rearrangement, and that the re-oxidation process would be achieved by closure of the photoredox catalytic loop (Scheme 2, Method 2; Scheme 3). In the case of both **2a** and **2b**, light irradiation in the presence of stoichiometric Ir(ppy)₂(dtbbpy)-PF₆ resulted in complete consumption of the helicate ¹H NMR signals and the appearance of **1a** and **1b** following 35 h and 4 days of irradiation using just a standard 42 W light bulb (Figures S17 and S19). In contrast, **2c** showed only very light change after nine days of irradiation (Figure S21). This difference in photoredox reactivity is likely caused by the lower kinetic lability of the Co^{II} species with bipy ligands (see above). With **2a–b**, the lack of the same conversion in the absence of light (Figures S18 and S20) and the quenching of the Ir(ppy)₂(dtbbpy)⁺ luminescence in the presence of the Co^{III} species both support a photoredox mechanism

that involves single electron transfer from the excited state of Ir^{III} to Co^{III}. The relative slow rate of these rearrangement reactions, even with stoichiometric Ir^{III} complex, is likely caused by a bimolecular mechanism that involves two mixed valence Co^{III}-Co^{II} species (Scheme 3) and the corresponding low steady state concentration of this species generated through the photoredox method.

Scheme 3. Proposed photoredox-induced assembly conversion mechanism.



The limitation of transforming one metallocupramolecular entity into another solely utilizing a stimuli that affects the thermodynamics of the system is that it is only possible to move energetically downhill. Thus we were keen to demonstrate it would also be possible to reconstitute a tetrahedron into a helicate, taking advantage of the ability to kinetically trap the system in a high energy state. Pleasingly, we have been able to successfully reconstitute both **1b** and **1c**—the more robust tetrahedra—into their corresponding, higher energy helicates, **2b** and **2c**. This was achieved by first unlocking with a stoichiometric amount of TBAI reductant, and then by rapidly re-locking the system via the rapid addition of CAN at elevated temperature (343 K) to trap the entropically smaller assembly. With this method we exclusively or overwhelmingly obtain the higher energy species, **2b** and **2c** (Scheme 2, Method 3; Figures S15 and S16).

Conclusions

The assembly-followed-by-fixing method we have exemplified here allows high-yielding access to structures not thermodynamically favored under “ambient” conditions. Furthermore, the wide and varied range of architectures that have previously been obtained using Co^{II} and different bridged bidentate ligands^{23d,e,j} and also the potential to explore more extreme “non-ambient” conditions (pressure, larger temperature ranges etc.) points to a very wide range of assemblies that are potentially attainable. It could be anticipated that these, like the ones presented here, will possess a kinetic stability not usually associated with many metal-organic ensembles. While there are other approaches to creating robust cage-type systems, notably the formation of fully covalent (organic) architectures,^{12,28} these systems generally lack the in-built mechanism whereby the structure can be (selectively) made labile using a simple redox (or photoredox)-based stimuli. These features, along with the recent report of hypoxic activation of Co^{III} pro-drugs³⁴ makes

water-soluble analogues of the capsules reported here²² prime candidates for biological testing. Such investigations using these and related systems are currently underway in our laboratory.

Experimental Methods

General. All reagents were purchased from commercial sources and used without further purification. All ¹H and ¹³C NMR spectra were recorded on either Bruker AV400, AV500, PRO500 or AV600 at a constant temperature of 300K unless stated otherwise. Chemical shifts are reported in parts per million from low to high field, referenced against values for the residual solvent peaks. Coupling constants (J) are reported as observed in Hz. Standard abbreviations indicating multiplicity were used as follows: m = multiplet, t = triplet, d = doublet, s = singlet, br(s/d) = broad (singlet/doublet etc.), appt = apparent triplet, etc. Mass spectrometry (ESI-MS) of all helicate and tetrahedron complexes was carried out using a Waters SYNAPT G2 instrument. The synthesis of **L^a** and **1a**·12PF₆ has been previously reported.¹⁹

Synthesis of 1b·12PF₆. To a suspension of **L^b** (0.0300 g, 60.9 μmol) in degassed acetonitrile (5.0 mL) was added cobalt(II) perchlorate hexahydrate (0.0149 g, 40.7 μmol), which after further degassing was heated at 50 °C for 1 h under an atmosphere of N₂. Once cooled to room temperature, cerium(IV) ammonium nitrate (0.0338 g, 61.6 μmol) in acetonitrile (5.4 mL) was added using a syringe pump at a rate of 25 μL/min. Once addition was complete, the precipitate was filtered onto celite, washed with acetonitrile, and then eluted with water-acetonitrile (2:1, 15.0 mL). The addition of ammonium hexafluorophosphate (0.797 g, 4.89 mmol) to the solution resulted in the formation of a precipitate, which was filtered onto celite, washed with water and then eluted in acetonitrile before the solvent was removed under vacuum to give the title compound as a red solid. Yield = 0.0389 g (78%). ¹H NMR (500 MHz, CD₃CN): δ 8.88 (d, *J* = 8.7 Hz, 12H, *m*-pyridyl-*H*), 8.81 (dd, *J* = 8.6, 1.8 Hz, 12H, *p*-pyridyl-*H*), 7.96 (d, *J* = 8.6 Hz, 12H, benzimidazole-*H*), 7.61 (ddd, *J* = 8.4, 7.3, 0.9 Hz, 12H, benzimidazole-*H*), 7.58 (d, *J* = 1.6 Hz, 12H, *o*-pyridyl-*H*), 7.49 (s, 24H, C₆H₄), 7.13 (ddd, *J* = 8.4, 7.2, 1.0 Hz, 12H, benzimidazole-*H*), 5.35 (d, *J* = 8.6 Hz, 12H, benzimidazole-*H*), 4.55 (s, 36H, N-CH₃). ¹³C NMR (126 MHz, CD₃CN): δ 151.6, 150.9, 146.1, 142.0, 141.5, 139.8, 138.6, 135.4, 129.1, 129.0, 128.7, 128.2, 115.4, 115.1, 35.2. ¹H DOSY NMR (500 MHz, CD₃CN): *D* = 4.73 × 10⁻⁶ cm² s⁻¹; calculated hydrodynamic radius = 12.5 Å. ESI-MS (*m/z*): 1087 (+4), 841 (+5), 676 (+6), 559 (+7), 471 (+8), 402 (+9) (see Supporting Information section 8 for expansions of each charge state and comparison with calculated isotopic distributions). Red crystals of **1b**·12PF₆ suitable for X-ray diffraction studies were grown by slow diffusion of diisopropyl ether into a saturated acetonitrile solution. X-ray analysis (CCDC 1425917) is detailed in Supporting Information section 9.

Synthesis of 1c·12PF₆. Following a similar method reported for **1b**·12PF₆ initially by adding cobalt(II) perchlorate hexahydrate (0.0136 g, 37.2 μmol) to a suspension of **L^c** (0.0215 g, 55.6 μmol) in acetonitrile (3.0 mL), the title compound was isolated as a yellow solid. Yield = 0.0307 g (77%). ¹H NMR (500 MHz, CD₃CN): δ 8.93 (d, *J* = 8.6 Hz, 12H, *endo*-*m*-pyridyl-*H*), 8.87 (dd, *J* = 8.5, 1.9 Hz, 12H, *endo*-*p*-pyridyl-*H*), 8.82 (dd, *J* = 8.2, 1.5 Hz, 12H, *exo*-*m*-pyridyl-*H*), 8.58-8.50

(m, 12H, *exo*-*p*-pyridyl-*H*), 7.82 (ddd, *J* = 7.6, 5.9, 1.4 Hz, 12H, *exo*-*m*-pyridyl-*H*), 7.46 (s, 24H, C₆H₄), 7.35 (d, *J* = 6.0 Hz, 12H, *exo*-*o*-pyridyl-*H*), 7.31 (d, *J* = 2.0 Hz, 12H, *endo*-*o*-pyridyl-*H*). ¹³C NMR (126 MHz, CD₃CN): δ 155.2, 154.7, 151.7, 148.0, 144.0, 141.3, 140.7, 134.3, 131.8, 128.0, 127.7, 126.9. ¹H DOSY NMR (500 MHz, CD₃CN): *D* = 4.90 × 10⁻⁶ cm² s⁻¹; calculated hydrodynamic radius = 12.1 Å. ESI-MS (*m/z*): 928 (+4), 713 (+5), 570 (+6), 468 (+7), 392 (+8), 332 (+9), 284 (+10), 245 (+11) (see Supporting Information section 8 for expansions of each charge state and comparison with calculated isotopic distributions).

Synthesis of 1d·12PF₆. Following a similar method reported for **1b**·12PF₆ initially by adding cobalt(II) perchlorate hexahydrate (0.0132 g, 36.1 μmol) to a suspension of **L^d** (0.0223 g, 53.8 μmol) in acetonitrile (2.9 mL), the title compound was isolated as a yellow solid. Yield = 0.0332 g (83%). ¹H NMR (500 MHz, CD₃CN): δ 8.74-8.70 (m, 24H, *exo*-*m*-pyridyl-*H* & *endo*-*m*-pyridyl-*H*), 8.54-8.49 (m, 12H, *exo*-*p*-pyridyl-*H*), 8.35 (dd, *J* = 8.4, 1.7 Hz, 12H, *endo*-*p*-pyridyl-*H*), 7.78 (ddd, *J* = 7.5, 5.9, 1.4 Hz, 12H, *exo*-*m*-pyridyl-*H*), 7.49 (d, *J* = 1.7 Hz, 12H, *endo*-*o*-pyridyl-*H*), 7.26 (dd, *J* = 6.0, 1.2 Hz, 12H, *exo*-*o*-pyridyl-*H*), 6.97 (s, 12H, C₆H₂(CH₃)₂), 1.88 (s, 36H, C₆H₂(CH₃)₂). ¹³C NMR (126 MHz, CD₃CN): δ 156.3, 155.8, 152.6, 150.5, 146.0, 145.2, 144.8, 136.5, 134.6, 133.1, 132.9, 128.7, 128.2, 20.3. ¹H DOSY NMR (500 MHz, CD₃CN): *D* = 4.75 × 10⁻⁶ cm² s⁻¹; calculated hydrodynamic radius = 12.4 Å. ESI-MS (*m/z*): 1341 (+3), 970 (+4), 747 (+5), 598 (+6), 350 (+9), 301 (+10), 260 (+11) (see Supporting Information section 8 for expansions of each charge state and comparison with calculated isotopic distributions). Yellow crystals of **1d**·12PF₆ suitable for X-ray diffraction studies were grown by slow diffusion of diisopropyl ether into a saturated acetonitrile solution. X-ray analysis (CCDC 1425919) is detailed in Supporting Information section 9.

Synthesis of 2a·6PF₆. **L^a** (0.0450 g, 78.9 μmol) was added to cobalt(II) perchlorate hexahydrate (0.0192 g, 52.5 μmol) in acetonitrile (500 mL), which was then heated for 1 h to ensure complete dissolution of the ligand. Once cooled to room temperature, cerium(IV) ammonium nitrate (0.0585 g, 106.7 μmol,) was added and the forming precipitate stirred for 0.5 h. The precipitate was then filtered onto celite, washed with acetonitrile, and then eluted with water-acetonitrile (2:1, 40 mL). The addition of ammonium hexafluorophosphate (1.03 g, 6.30 mmol) to the solution resulted in the formation of a precipitate, which was filtered onto celite, washed with water and then dissolved in acetonitrile before the solvent was removed under vacuum to give the title compound as an orange solid. Yield = 0.0659 g (93%). ¹H NMR (500 MHz, CD₃CN): δ 9.11 (s, 6H, triazole-*H*), 8.78 (d, *J* = 8.2 Hz, 6H, *p*-pyridyl-*H*), 8.55 (d, *J* = 8.2 Hz, 6H, *m*-pyridyl-*H*), 7.34 (s, 12H, C₆H₄), 6.71 (s, 6H, *o*-pyridyl-*H*), 4.83-4.69 (m, 12H, peg-*H*), 3.93(t, *J* = 4.8 Hz, 12H, peg-*H*), 3.67-3.59 (m, 12H, peg-*H*), 3.52-3.46 (m, 12H, peg-*H*), 3.30 (s, 18H, pegOCH₃). ¹³C NMR (126 MHz, CD₃CN): δ 150.1, 150.0, 148.7, 142.8, 141.9, 136.6, 129.7, 129.4, 127.4, 72.4, 71.0, 68.9, 59.0, 55.2. ¹H DOSY NMR (500 MHz, CD₃CN): *D* = 5.94 × 10⁻⁶ cm² s⁻¹; calculated hydrodynamic radius = 10.0 Å. ESI-MS (*m/z*): 1204 (+2), 754 (+3), 529 (+4), 394 (+5) (see Supporting Information section 8 for expansions of each charge state and comparison with calculated isotopic distributions).

Synthesis of 2b·6PF₆. Following a similar method reported for **2a**·6PF₆ starting with **L^b** (0.0543 g, 110 μmol) and

cobalt(II) perchlorate hexahydrate (0.0269 g, 73.5 μmol) in acetonitrile (950 mL), the title compound was isolated as a red solid. Yield = 0.0421 g (93%). ^1H NMR (500 MHz, CD_3CN): δ 8.94–8.89 (m, 12H, *p*-pyridyl-*H* & *m*-pyridyl-*H*), 8.03 (d, J = 8.6 Hz, 6H, benzimidazole-*H*), 7.69 (appt, 6H, benzimidazole-*H*), 7.39 (s, 12H, C_6H_4), 7.21 (appt, 6H, benzimidazole-*H*), 6.49 (br s, 6H, *o*-pyridyl-*H*), 5.41 (d, J = 8.6 Hz, 6H, benzimidazole-*H*), 4.60 (s, 18H, N- CH_3). ^{13}C NMR (126 MHz, CD_3CN): δ 151.3, 151.1, 148.0, 142.1, 141.7, 140.0, 138.3, 135.9, 129.8, 129.3, 129.1, 128.8, 115.4, 115.4, 35.2. ^1H DOSY NMR (500 MHz, CD_3CN): D = $6.41 \times 10^{-6} \text{ cm}^2 \text{ s}^{-1}$; calculated hydrodynamic radius = 9.2 Å. ESI-MS (m/z): 676 (+3), 471 (+4), 348 (+5), 266 (+6) (see Supporting Information section 8 for expansions of each charge state and comparison with calculated isotopic distributions).

Synthesis of 2c·6PF₆. Following a similar method reported for 2a·6PF₆ starting with L^c (0.0419 g, 108 μmol) and cobalt(II) perchlorate hexahydrate (0.0265 g, 72.4 μmol) in acetonitrile (1 L), the title compound was isolated as a yellow solid. Yield = 0.0639 g (82%). ^1H NMR (500 MHz, CD_3CN): δ 8.90–8.86 (m, 12H, *endo-p*-pyridyl-*H* & *endo-m*-pyridyl-*H*), 8.82 (dd, J = 8.1, 1.1 Hz, 6H, *exo-m*-pyridyl-*H*), 8.64–8.57 (m, 6H, *exo-p*-pyridyl-*H*), 7.90 (ddd, J = 7.6, 6.0, 1.4 Hz, 6H, *exo-m*-pyridyl-*H*), 7.35 (s, 12H, C_6H_4), 7.31 (dd, J = 6.0, 0.7 Hz, 6H, *exo-o*-pyridyl-*H*), 6.34 (br s, 6H, *endo-o*-pyridyl-*H*). ^{13}C NMR (126 MHz, CD_3CN): δ 156.1, 156.1, 151.7, 148.6, 144.1, 142.0, 141.0, 135.0, 132.0, 128.4, 128.2, 127.9. ^1H DOSY NMR (500 MHz, CD_3CN): D = $6.48 \times 10^{-6} \text{ cm}^2 \text{ s}^{-1}$; calculated hydrodynamic radius = 9.2 Å. ESI-MS (m/z): 570 (+3), 391 (+4), 284 (+5), 212 (+6) (see Supporting Information section 8 for expansions of each charge state and comparison with calculated isotopic distributions). Yellow crystals of 2c·6BF₄ (prepared by adding NaBF₄ at ion metathesis stage) suitable for X-ray diffraction studies were grown by slow diffusion of diisopropyl ether into a saturated acetonitrile solution. X-ray analysis (CCDC 1425918) is detailed in Supporting Information section 9.

Synthesis of 2d·6PF₆. Following a similar method reported for 2a·6PF₆ starting with L^d (0.0109 g, 26.3 μmol) and cobalt(II) perchlorate hexahydrate (0.0064 g, 17.5 μmol) in acetonitrile (500 mL), the title compound was isolated as an orange solid. Yield = 0.0063 g (64%). ^1H NMR (500 MHz, CD_3CN): δ 8.88 (d, J = 8.5 Hz, 6H, *endo-m*-pyridyl-*H*), 8.81 (dd, J = 8.1, 1.5 Hz, 6H, *exo-m*-pyridyl-*H*), 8.78 (dd, J = 8.4, 1.8 Hz, 6H, *endo-p*-pyridyl-*H*), 8.65–8.55 (m, 6H, *exo-p*-pyridyl-*H*), 7.89 (ddd, J = 7.7, 6.0, 1.5 Hz, 6H, *exo-m*-pyridyl-*H*), 7.23 (s, 6H, $\text{C}_6\text{H}_2(\text{CH}_3)_2$), 7.10 (dd, J = 6.1, 1.3 Hz, 6H, *exo-o*-pyridyl-*H*), 6.81 (d, J = 1.9 Hz, 6H, *endo-o*-pyridyl-*H*), 1.74 (s, 18H, $\text{C}_6\text{H}_2(\text{CH}_3)_2$). ^{13}C NMR (126 MHz, CD_3CN): δ 156.8, 156.3, 152.9, 149.6, 145.4, 144.2, 144.1, 135.4, 135.3, 133.4, 129.0, 129.0, 19.4. ^1H DOSY NMR (500 MHz, CD_3CN): D = $6.33 \times 10^{-6} \text{ cm}^2 \text{ s}^{-1}$; calculated hydrodynamic radius = 9.3 Å. ESI-MS (m/z): 970 (+2), 598 (+3), 412 (+4), 301 (+5), 226 (+6) (see Supporting Information section 8 for expansions of each charge state and comparison with calculated isotopic distributions). Yellow crystals of 2d·6BF₄ (prepared by adding NaBF₄ at ion metathesis stage) suitable for X-ray diffraction studies were grown by slow diffusion of diisopropyl ether into a saturated acetonitrile solution. X-ray analysis (CCDC 1429784) is detailed in Supporting Information section 9.

ASSOCIATED CONTENT

Supporting Information. Synthetic procedures and characterization of L^{b-d}, ^1H and ^{13}C NMR spectra of all new compounds, MS of all coordination assemblies, Co^{II} equilibrium experiments, variable oxidation rate studies, helicate stability experiments, redox and photoredox switching protocols, X-ray crystallographic details. Crystallographic data have been deposited with the Cambridge Crystallographic Data Centre as entries CCDC 1425917 (1b·12PF₆), CCDC 1425919 (1d·12PF₆), CCDC 1425918 (2c·6BF₄) and 1429784 (2d·6BF₄).

AUTHOR INFORMATION

Corresponding Author

* Correspondence should addressed to Paul.Lusby@ed.ac.uk.

Author Contributions

All authors have given approval to the final version of the manuscript.

Notes

The authors declare no competing financial interests.

ACKNOWLEDGMENT

This work was supported by the UK Engineering and Physical Sciences Research Council (EPSRC). We thank Dr. Euan R. Kay (University of St. Andrews) for useful discussions.

REFERENCES

- (1) (a) Pascu, G. I.; Hotze, Anna C. G.; Sanchez-Cano, C.; Kariuki, B. M.; Hannon, M. J. *Angew. Chem. Int. Ed.* **2007**, *46*, 4374; (b) Therrien, B.; Suess-Fink, G.; Govindaswamy, P.; Renfrew, A. K.; Dyson, P. J. *Angew. Chem. Int. Ed.* **2008**, *47*, 3773; (c) Faulkner, A. D.; Kaner, R. A.; Abdallah, Q. M. A.; Clarkson, G.; Fox, D. J.; Gurnani, P.; Howson, S. E.; Phillips, R. M.; Roper, D. I.; Simpson, D. H.; Scott, P. *Nature Chem.* **2014**, *6*, 797; (d) Grishagin, I. V.; Pollock, J. B.; Kushal, S.; Cook, T. R.; Stang, P. J.; Olenyuk, B. Z. *Proc. Natl Acad. Sci. USA* **2014**, *111*, 18448; (e) McNeill, S. M.; Preston, D.; Lewis, J. E. M.; Robert, A.; Knerr-Rupp, K.; Graham, D. O.; Wright, J. R.; Giles, G. I.; Crowley, J. D. *Dalton Trans.* **2015**, *44*, 11129.
- (2) (a) Kang, J.; Santamaria, J.; Hilmersson, G.; Rebek, J. J. *Am. Chem. Soc.* **1998**, *120*, 7389; (b) Merlau, M. L.; Mejia, M. d. P.; Nguyen, S. T.; Hupp, J. T. *Angew. Chem. Int. Ed.* **2001**, *40*, 4239; (c) Slagt, V. F.; Reek, J. N. H.; Kamer, P. C. J.; van Leeuwen, P. W. N. M. *Angew. Chem. Int. Ed.* **2001**, *40*, 4271; (d) Yoshizawa, M.; Tamura, M.; Fujita, *Science* **2006**, *312*, 251; (e) Pluth, M. D.; Bergman, R. G.; Raymond, K. N. *Science*, **2007**, *316*, 85; (f) Yoon, H. J.; Kuwabara, J.; Kim, J.-H.; Mirkin, C. A. *Science*, **2010**, *330*, 66; (g) Hastings, C. J.; Pluth, M. D.; Bergman, R. G.; Raymond, K. N. *J. Am. Chem. Soc.* **2010**, *132*, 6938; (h) Salles, A. G.; Zarra, S.; Turner, R. M.; Nitschke, J. R. *J. Am. Chem. Soc.* **2013**, *135*, 19143; (i) Kaphan, D. M.; Levin, M. D.; Bergman, R. G.; Raymond, K. N.; Toste, F. D. *Science*, **2015**, *350*, 1235; (j) Cullen, W.; Misuraca, M. C.; Hunter, C. A.; Williams, N. H.; Ward, M. D. *Nature Chem.* **2016**, *8*, 231; (k) Wang, Q.-Q.; Gonell, S.; Leenders, S. H. A. M.; Dürr, M.; Ivanović-Burmazović, I.; Reek, J. N. H. *Nature Chem.* **2016**, *8*, 225.
- (3) (a) Yoshizawa, M.; Kusukawa, T.; Fujita, M.; Yamaguchi, K. *J. Am. Chem. Soc.* **2000**, *122*, 6311; (b) Mal, P.; Breiner, B.; Rissanen, K.; Nitschke, J. R. *Science*, **2009**, *324*, 1697; (c) Liu, Y.; Hu, C.; Comotti, A.; Ward, M. D. *Science* **2011**, *333*, 436.
- (4) While the vast majority of self-assembly reactions are under overall (reversible) thermodynamic control, some often display significant levels of cooperativity that direct the self-assembly reaction down a particular (kinetic) pathway. The hallmark of a kinetically controlled self-assembly reaction is often the sensitivity to the sequence of addition of components. For a very elegant example of this, see: Levin, M. D.; Stang, P. J. *J. Am. Chem. Soc.* **2000**, *122*, 7428.

- (5) (a) Dalgarno, S. J.; Power, N. P.; J. L. Atwood, *Coord. Chem. Rev.* **2008**, 252, 825; (b) Chakrabarty, R.; Mukherjee, P. S.; Stang, P. J. *Chem. Rev.* **2011**, 111, 6810; (c) Mukherjee, S.; Mukherjee, P. S. *Chem. Commun.* 2014, 50, 2239; (d) Cook, T. R.; Stang, P. J. *Chem. Rev.* **2015**, 115, 7001.
- (6) (a) Fujita, M.; Sasaki, O.; Mitsunashi, T.; Fujita, T.; Yazaki, J.; Yamaguchi, K.; Ogura, K. *Chem. Commun.* **1996**, 1535; (b) Schweiger, M.; Seidel, S. R.; Arif, A. M.; Stang, P. J. *Inorg. Chem.* **2002**, 41, 2556; (c) Cotton, F. A.; Murillo, C. A.; Yu, R. *Dalton Trans.* **2006**, 3900.
- (7) Riddell, I. A.; Ronson, T. K.; Clegg, J. K.; Wood, C. S.; Bilbeisi, R. A.; Nitschke, J. R. *J. Am. Chem. Soc.* **2014**, 136, 9491.
- (8) (a) Hunter, C. A.; Anderson, H. L. *Angew. Chem. Int. Ed.* **2009**, 48, 7488. For example of chelate cooperativity in coordination assemblies, see (b) Sato, S.; Ishido, Y.; Fujita, M. *J. Am. Chem. Soc.* **2009**, 131, 6064; (c) Henkelis, J. J.; Fisher, J.; Warriner, S. L.; Hardie, M. J. *Chem. Eur. J.* **2014**, 20, 4117.
- (9) Thomas, J. A. *Chem. Soc. Rev.* **2007**, 36, 856.
- (10) For reviews on DCC, see (a) Corbett, P. T.; Leclaire, J.; Vial, L.; West, K. R.; Wietor, J.-L.; Sanders, J. K. M.; Otto, S. *Chem. Rev.* **2006**, 106, 3652; (b) Jin, Y.; Yu, C.; Denman, R. J.; Zhang, W. *Chem. Soc. Rev.* **2013**, 42, 6634.
- (11) (a) Hamilton, D. G.; Feeder, N.; Teat, S. J.; Sanders, J. K. M. *New J. Chem.* **1998**, 1019; (b) Kidd, T. J.; Leigh, D. A.; Wilson, A. J.; *J. Am. Chem. Soc.* **1999**, 121, 1599; (c) Glink, P. T.; Oliva, A. I.; Stoddart, J. F.; White, A. J. P.; Williams, D. J. *Angew. Chem. Int. Ed.* **2001**, 40, 1870; (d) Kilbinger, A. F. M.; Cantrill, S. J.; Waltman, A. W.; Day, M. W.; Grubbs, R. H. *Angew. Chem. Int. Ed.* **2003**, 42, 3281; (e) Hogg, L.; Leigh, D. A.; Lusby, P. J.; Morelli, A.; Parsons, S.; Wong, J. K. Y. *Angew. Chem. Int. Ed.* **2004**, 43, 1218; (f) Peters, A. J.; Chichak, K. S.; Cantrill, S. J.; Stoddart, J. F. *Chem. Commun.* **2005**, 3394; (g) Lam, R. T. S.; Belenguer, A.; Roberts, S. L.; Naumann, C.; Jarrosson, T.; Otto, S.; Sanders, J. K. M. *Science* **2005**, 308, 667; (h) West, K. R.; Ludlow, R. F.; Corbett, P. T.; Besenius, P.; Mansfeld, F. M.; Cormack, P. A. G.; Sherrington, D. C.; Goodman, J. M.; Stuart, M. C. A.; Otto, S. *J. Am. Chem. Soc.* **2008**, 130, 10834; (i) Wood, C. S.; Ronson, T. K.; Belenguer, A. M.; Holstein, J. J.; Nitschke, J. R. *Nature Chem.* **2015**, 7, 354.
- (12) (a) Liu, X.; Liu, Y.; Li, G.; Warmuth, R. *Angew. Chem. Int. Ed.* **2006**, 45, 901; (b) Christinat, N.; Scopelliti, R.; Severin, K. *Angew. Chem. Int. Ed.* **2008**, 47, 1848; (c) Hiraoka, S.; Yamauchi, Y.; Arakane, R.; Shionoya, M. *J. Am. Chem. Soc.* **2009**, 131, 11646; (d) Swamy, S. I.; Bacsa, J.; Jones, J. T. A.; Stylianou, K. C.; Steiner, A.; Ritchie, L. K.; Hasell, T.; Gould, J. A.; Laybourn, A.; Khimyak, Y. Z.; Adams, D. J.; Rosseinsky, M. J.; Cooper, A. I. *J. Am. Chem. Soc.* **2010**, 132, 12773; (e) Zhang, C.; Wang, Q.; Long, H.; Zhang, W. *J. Am. Chem. Soc.* **2011**, 133, 20995; (f) Asadi, A.; Ajami, D.; Rebek, J. *Chem. Sci.* **2013**, 4, 1212; (g) Mosquera, J.; Zarra, S.; Nitschke, J. R. *Angew. Chem. Int. Ed.* **2014**, 53, 1556.
- (13) (a) von Delius, M.; Geertsema, E. M.; Leigh, D. A. *Nature Chem.* **2010**, 2, 96; (b) Kovářiček, P.; Lehn, J.-M. *Chem. Eur. J.* **2015**, 21, 9380; (c) Kassem, S.; Lee, A. T. L.; Leigh, D. A.; Markevicius, A.; Solà, J. *Nature Chem.* **2016**, 3, 138.
- (14) (a) Davis, A. V.; Raymond, K. N. *J. Am. Chem. Soc.* **2005**, 127, 7912; (b) Cangelosi, V. M.; Carter, T. G.; Zakharov, L. N.; Johnson, D. W. *Chem. Commun.* **2009**, 5606.
- (15) For examples which rely on the high temperature labilization of 2nd and 3rd row transition-metal ion-ligand interactions, see to (a) Fujita, M.; Ibukuro, F.; Hagihara, H.; Ogura, K.; *Nature* **1994**, 367, 720; (b) Fujita, M.; Ibukuro, F.; Yamaguchi, K.; Ogura, K. *J. Am. Chem. Soc.* **1995**, 117, 4175; (c) Ibukuro, F.; Kusakawa, T.; Fujita, M. *J. Am. Chem. Soc.* **1998**, 120, 8561; (d) Roche, S.; Haslam, C.; Heath, S. L.; Thomas, J. A. *Chem. Commun.* **1998**, 1681; (e) Glasson, C. R. K.; Meehan, G. V.; Clegg, J. K.; Lindoy, L. F.; Smith, J. A.; Keene, F. R.; Motti, C. *Chem. Eur. J.* **2008**, 14, 10535. For examples which utilize a combination of fixed and labile metal-ligand interactions, see (f) Newkome, G. R.; Wang, P.; Moorefield, C. N.; Cho, T. J.; Mohapatra, P. P.; Li, S.; Hwang, S.-H.; Lukyanova, O.; Echegoyen, L.; Palagallo, J. A.; Iancu, V.; Hla, S.-W. *Science*, **2006**, 312, 1782; (g) Chepelin, O.; Ujma, J.; Barran, P. E.; Lusby, P. J. *Angew. Chem. Int. Ed.* **2012**, 51, 4194; (h) Metherell, A. J.; Ward, M. D. *Chem. Sci.* **2016**, 7, 910. Appropriate “spectator” ligands can dramatically labilize exchangeable 2nd and 3rd row M–L interactions, permitting self-assembly under ambient conditions, see (i) Leininger, S.; Fan, J.; Schmitz, M.; Stang, P. J. *Proc. Natl Acad. Sci. USA* **2000**, 97, 1380; (j) Chepelin, O.; Ujma, J.; Wu, X.; Slawin, A. M. Z.; Pitak, M. B.; Coles, S. J.; Michel, J.; Jones, A. C.; Barran, P. E.; Lusby, P. J. *J. Am. Chem. Soc.* **2012**, 134, 19334.
- (16) Tashiro, S.; Tominaga, M.; Kusakawa, T.; Kawano, M.; Sakamoto, S.; Yamaguchi, K.; Fujita, M. *Angew. Chem. Int. Ed.* **2003**, 42, 3267.
- (17) Fujita, D.; Takahashi, A.; Sato, S.; Fujita, M. *J. Am. Chem. Soc.* **2011**, 133, 13317.
- (18) (a) Yamashita, K.; Kawano, M.; Fujita, M. *J. Am. Chem. Soc.* **2007**, 129, 1850; (b) Yamashita, K.; Sato, K.; Kawano, M.; Fujita, M. *New J. Chem.* **2009**, 33, 264.
- (19) Symmers, P. R.; Burke, M. J.; August, D. P.; Thomson, P. I. T.; Nichol, G. S.; Warren, M. R.; Campbell, C. J.; Lusby, P. J. *Chem. Sci.* **2015**, 6, 756.
- (20) (a) Charbonniere, L. J.; Bernardinelli, G.; Piguat, C.; Sargeson, A. M.; Williams, A. F. *J. Chem. Soc., Chem. Commun.* **1994**, 1419; (b) Leigh, D. A.; Lusby, P. J.; McBurney, R. T.; Morelli, A.; Slawin, A. M. Z.; Thomson, A. R.; Walker, D. B. *J. Am. Chem. Soc.* **2009**, 131, 3762; (c) Mugesana, C.; Guillet, P.; Hoepfener, S.; Schubert, U. S.; Fustin, C.-A.; Gohy, J.-F. *Chem. Commun.* **2010**, 46, 1296; (d) Constable, E. C.; Harris, K.; Housecroft, C. E.; Neuburger, M. *Dalton Trans.* **2011**, 40, 1524; (e) Ayme, J.-F.; Lux, J.; Sauvage, J.-P.; Sour, A. *Chem. Eur. J.* **2012**, 18, 5565. For a similar use of Cr^{II}/Cr^{III}, see (f) Cantuel, M.; Bernardinelli, G.; Imbert, D.; Bünzli, J.-C. G.; Hopfgartner, G.; Piguat, C. *J. Chem. Soc., Dalton Trans.* **2002**, 1929.
- (21) With rigid, bis(bidentate) ligands and metal ions with strong octahedral preference, M₂L₃ helicates are generally only observed as minor equilibrium components, see (a) Glasson, C. R. K.; Meehan, G. V.; Motti, C. A.; Clegg, J. K.; Turner, P.; Jensen, P.; Lindoy, L. F. *Dalton Trans.* **2011**, 40, 10481; (b) Ousaka, N.; Grunder, S.; Castilla, A. M.; Whalley, A. C.; Stoddart, J. F.; Nitschke, J. R. *J. Am. Chem. Soc.* **2012**, 134, 15528. With non-labile octahedral metal ions e.g. Ru^{II}, M₂L₃ helicates can be obtained in low yields using rigid ligands, suggesting these are kinetically trapped intermediates (see ref 15e).
- (22) (a) Hernandez, J. V.; Kay, E. R.; Leigh, D. A. *Science* **2004**, 306, 1532; (b) Cheng, C.; McGonigal, P. R.; Liu, W.-G.; Li, H.; Vermeulen, N. A.; Ke, C.; Frascioni, M.; Stern, C. L.; Goddard, W. A.; Stoddart, J. F. *J. Am. Chem. Soc.* **2014**, 136, 14702; (c) Ragazzon, G.; Baroncini, M.; Silvi, S.; Venturi, M.; Credi, A. *Nature Nanotech.* **2015**, 10, 70.
- (23) (a) Scherer, M.; Caulder, D. L.; Johnson, D. W.; Raymond, K. N. *Angew. Chem. Int. Ed.* **1999**, 38, 1588; (b) Xu, J.; Parac, T. N.; Raymond, K. N. *Angew. Chem. Int. Ed.* **1999**, 38, 2878; (c) Beissel, T.; Powers, R. E.; Parac, T. N.; Raymond, K. N. *J. Am. Chem. Soc.* **1999**, 121, 4200; (d) Stephenson, A.; Argent, S. P.; Riis-Johannessen, T.; Tidmarsh, I. S.; Ward, M. D. *J. Am. Chem. Soc.* **2011**, 133, 858; (e) Riddell, I. A.; Smulders, M. M. J.; Clegg, J. K.; Hristova, Y. R.; Breiner, B.; Thoburn, J. D.; Nitschke, J. R. *Nature Chem.* **2012**, 4, 751; (f) Zarra, S.; Clegg, J. K.; Nitschke, J. R. *Angew. Chem. Int. Ed.* **2013**, 52, 4837; (g) Meng, W.; Ronson, T. K.; Clegg, J. K.; Nitschke, J. R. *Angew. Chem. Int. Ed.* **2013**, 52, 1017; (h) Young, M. C.; Johnson, A. M.; Gamboa, A. S.; Hooley, R. J. *Chem. Commun.* **2013**, 49, 1627; (i) Young, M. C.; Holloway, L. R.; Johnson, A. M.; Hooley, R. J. *Angew. Chem., Int. Ed.* **2014**, 53, 9832; (j) Cullen, W.; Hunter, C. A.; Ward, M. D. *Inorg. Chem.* **2015**, 54, 2626.
- (24) \sum the sum of the absolute deviations from 90° of the 12 cis angles, is averaged at 45° for **2c** and 41° for **2d**. The twist angles are $\theta = 55^\circ$ (**2c**) and 54° (**2d**) [$0^\circ =$ ideal trigonal prismatic; $60^\circ =$ ideal octahedral].
- (25) (a) Seeber, G.; Tiedemann, B. E. F.; Raymond, K. N. *Top. Curr. Chem.* **2006**, 265, 147; (b) Castilla, A. M.; Ramsay, W. J.; Nitschke, J. R. *Chem. Lett.* **2014**, 43, 256.
- (26) (a) Fujita, N.; Biradha, K.; Fujita, M.; Sakamoto, S.; Yamaguchi, K. *Angew. Chem. Int. Ed.* **2001**, 40, 1718; (b) Hiraoka, S.; Harano, K.; Shiro, M.; Shionoya, M. *Angew. Chem. Int. Ed.* **2005**, 44, 2727; (c) Hiraoka, S.; Sakata, Y.; Shionoya, M. *J. Am. Chem. Soc.* **2008**, 130, 10058; (d) Zhao, L.; Northrop, B. H.; Stang, P. J. *J. Am. Chem. Soc.* **2008**, 130, 11886; (e) Oliveri, C. G.; Ulmann, P. A.; Wiester, M. J.;

- Mirkin, C. A. *Acc. Chem. Res.* **2008**, *41*, 1618; (f) Aimi, J.; Nagamine, Y.; Tsuda, A.; Muranaka, A.; Uchiyama, M.; Aida, T. *Angew. Chem. Int. Ed.* **2008**, *47*, 5153; (g) Kilbas, B.; Mirtschin, S.; Scopelliti, R.; Severin, K. *Chem. Sci.* **2012**, *3*, 701-704; (h) Yi, S.; Brega, V.; Captain, B.; Kaifer, A. E. *Chem. Commun.* **2012**, *48*, 10295; (i) Neogi, S.; Lorenz, Y.; Engeser, M.; Samanta, D.; Schmittel, M. *Inorg. Chem.* **2013**, *52*, 6975; (j) Stadler, A.-M.; Burg, C.; Ramirez, J.; Lehn, J.-M. *Chem. Commun.* **2013**, *49*, 5733; (k) Lu, X.; Li, X.; Guo, K.; Xie, T.-Z.; Moorefield, C. N.; Wesdemiotis, C.; Newkome, G. R. *J. Am. Chem. Soc.* **2014**, *136*, 18149; (l) Zhu, R.; Luebben, J.; Dittrich, B.; Clever, G. H. *Angew. Chem. Int. Ed.* **2015**, *54*, 2796; (m) Jurček, O.; Bonakdarzadeh, P.; Kalenius, E.; Linnanto, J. M.; Groessl, M.; Knochenmuss, R.; Ihalainen, J. A.; Rissanen, K. *Angew. Chem. Int. Ed.* **2015**, *54*, 15462; (n) Preston, D.; Fox-Charles, A.; Lo, W. K. C.; Crowley, J. D. *Chem. Commun.* **2015**, *51*, 9042; (o) Han, M.; Luo, Y.; Damaschke, B.; Gómez, L.; Ribas, X.; Jose, A.; Peretzki, P.; Seibt, M.; Clever, G. H. *Angew. Chem. Int. Ed.* **2016**, *55*, 445. For a recent redox-induced metal-supramolecular disassembly-reassembly process, see (p) Croué, V.; Goeb, S.; Szalóki, G.; Allain, M.; Sallé, M. *Angew. Chem. Int. Ed.* **2016**, *55*, 1746.
- (27) (a) Nicewicz, D. A.; MacMillan, D. W. C. *Science* **2008**, *322*, 77; (b) Narayanam, J. M. R.; Stephenson, Corey R. J. *Chem. Soc. Rev.* **2011**, *40*, 102; (c) For an early example of photoredox catalysis using inexpensive Cu phenanthroline complexes, see (c) Kern, J.-M.; Sauvage, J.-P. *J. Chem. Soc. Chem. Commun.* **1987**, 546.
- (28) (a) Tanner, M. E.; Knobler, C. B.; Cram, D. J. *J. Am. Chem. Soc.* **1990**, *112*, 1659; (b) Kang, B.; Kurutz, J. W.; Youm, K.-T.; Totten, R. K.; Hupp, J. T.; Nguyen, S. T. *Chem. Sci.* **2012**, *3*, 1938; (c) Liu, S.; Russell, D. H.; Zinnel, N. F.; Gibb, B. C. *J. Am. Chem. Soc.* **2013**, *135*, 4314; (d) Dale, E. J.; Vermeulen, N. A.; Thomas, A. A.; Barnes, J. C.; Juricek, M.; Blackburn, A. K.; Strutt, N.L.; Sarjeant, A. A.; Stern, C. L.; Denmark, S. E.; Stoddart, J. F. *J. Am. Chem. Soc.* **2014**, *136*, 10669.
- (29) Karthaler-Benbakka, C.; Groza, D.; Kryeziu, K.; Pichler, V.; Roller, A.; Berger, W.; Heffeter, P.; Kowol, C. R. *Angew. Chem. Int. Ed.* **2014**, *53*, 12930.

